Med. & Biol. Eng. & Comput., 1980, 18, 271–280

Cardiac assessment mechanics: 1 Left ventricular mechanomyocardiography, a new approach to the detection of diseased myocardial elements and states

D. N. Ghista

Department of Mechanical Engineering-Engineering Mechanics, Michigan Technological University, Houghton, Michigan 49931, USA

G. Ray

Mechanical Engineering Department, Southern University, Baton Rouge, Louisiana 70813, USA

H. Sandler

Biomedical Research Division, NASA, Ames Research Centre, Moffett Field, California 94035, USA

Abstract—*The inadequacies of currently employed methods for assessment of cardiac mechanics are discussed, and the need for development of more intrinsic assessment parameters is emphasised. To this end, a new technique is presented to enable determination of regional mechanical constitutive properties of the myocardium during diastole; this technique has been originally named left-ventricular mechanomyocardiography (or l.v.-m.m.c.g.). The data required for implementation of the techniques consist of left-ventricular sequential dynamic geometry and associated recorded chamber pressure. The method entails matching of the inner-boundary deformations of the instantaneous finite-element model of the left ventricle (which is loaded by the recorded instantaneous incremental pressure) with the actual instantaneous endocardial deformations (as derived from either cineangiocardiography or 2-dimensional echocardiography), to determine the regional distribution of the Young's modulus E_{ne} and the incremental stresses $\Delta\sigma_{ne}$ (and hence the total stress $\sigma_{ne} = \Sigma_n \Delta\sigma_{ne}$) of the myocardial elements. The mechanical constitutive properties of the myocardial elements can be then characterised by the constitutive relation $E_{ne} = a + b\sigma_{ne}$. The constitutive parameters a and b have typical ranges for normal and pathological (ischaemic and infarcted) myocardial elements and hence can be employed to distinguish diseased elements. The values of a and b are calculated for normal and pathological subjects and their normal and pathological ranges are presented.*

1 Introduction

THE heart is a neuroelectrically actuated mechanical pump. The electrical potential generation and conduction properties govern the myocardial mechanical constitutive properties and the chamber wall motion, that in turn help develop the pressure and flow patterns in the cardiac chamber, which then influence the blood pressure and flow rate in the outflow tract. The aetiology of cardiac dysfunction can be attributed to either an actuation mechanism abnormality or to coronary artery disease (and associated myocardial damage), or to congenital shunts and anomalous cardiopulmonary vasculature or to vascular pathology (and malfunction), all of which affect its efficiency, and hence its function to maintain appropriate blood flow and pressure.

Noninvasive techniques are no doubt available for assessing the abnormalities in electrical potential generation and conduction. To this end, inverse-electrocardiography now enables us to determine the activation patterns (BAKER and PILKINGTON, 1974).

On the other hand, nuclear cardiography and scintigraphy techniques help provide detection of shunts, anomalous cardiopulmonary vasculature and diseased myocardium by means of regional myocardial perfusion and regional myocardial blood-flow determination (HARRISON *et al.*, 1975). For instance, thallium–201 is taken by the normal myocardium leaving a defect in the area of myocardial infarction, while ^{99m}Tc Pyrophosphate is taken up by the infarcted myocardium giving a 'hot' image. Likewise, the regional washout of intracoronary injected xenon–133, by precardial counting, provides regional myocardial blood-flow rates.

We will concentrate, in the framework of this paper, on the evaluation of the mechanical function of the heart and, in essence, the left ventricle. In this context, let us delineate the diagnostically relevant system variables and the intrinsic parameters that are responsible for these variables.

The cardiac chambers synchronise their filling, myocardial contraction, ejection and myocardial relaxation activities. The net effect of these activities is the generation of blood pressure–volume in the

First received 13th August 1978 and in final form 30th July 1979

0140–0118/80/030271-10 $01·50/0

chamber and blood pressure-flow rate in the outflow tracts. These so-called hydraulic variables represent the system variables, which are most relevant from a clinical cardiology standpoint. Hence, their determination constitutes a major (and traditional) area of activity in 'assessment cardiac mechanics'.

For prognostic and treatment guidelines, however, it is more advantageous for detecting the aetiology of cardiac pathology (as inferred by the above-mentioned system variables), to determine the more intrinsic factors which in fact are responsible for the (macro) hydraulic variables output. These factors are (i) the regional elastic properties of the myocardium and the heart valves, and, more illustratively, (ii) the resulting pressure and velocity patterns in the left ventricular chamber. The determination of these parameters constitutes a new approach to 'assessment cardiac mechanics', which we wish to advocate. In this paper (part 1) we will present the determination of the regional elastic properties of the myocardium, and their physiological relevance. In part 2, we will provide the theoretical and experimental evaluation of the left ventricular chambers, blood pressure distribution and patterns, as an index of left-ventricular pumping efficiency.

2 Some major available approaches for the determination of left ventricular myocardial properties from cardiac catheterisation data

2.1 *Models for determining the effective modulus of the left ventricle*

A number of models exist that enable determination of the so called effective modulus of the left ventricle. In 1969 VAYO and GHISTA and GHISTA *et al.* (1975*a*) determined this instantaneous effective left-ventricle modulus (throughout the cardiac cycle) by matching (i) the wall strains of their elasticity ellipsoidal-shaped model, calculated in terms of the known instantaneous chamber pressure and geometry and the unknown modulus, with (ii) the instantaneous left-ventricular strains obtained from cineangiographically derived sequential chamber geometrical data.

In another approach, GHISTA *et al.* (1975*b*) determined the effective left-ventricular modulus at the instants of occurrence of first and third heart sounds (i.e. both during diastole and systole) by matching the frequency expression of an equivalent left ventricular spherical model (obtained as a function of the known instantaneous chamber dimensions and the to-be-determined modulus) with the associated dominant heart sound frequency (obtained from a spectral analysis of that heart sound).

For both the above mentioned elasticity and vibrational modes of the left ventricle, some physiological and clinical correlations (such as characterisation of cardiomyopathy, left-ventricular compensation to pressure-volume overload and ensuing dilatation) of the results were demonstrated. Following on from these studies, PAO *et al.* (1977) recently used a finite-element model to demonstrate the evaluation of global effective modulus (averaged during diastole) by matching the expression for the strain energy stored during diastole (obtained as a function of the known left-ventiricular geometry and unknown modulus) with the monitored strain energy from the pressure-volume curve. The diagnostic utility of such a global diastolic modulus is minimal (since the Young's modulus is time or chamber pressure or myocardial stress dependent), as is also the case with studies concerning evaluation of myocardial stress.

MIRSKY (1973), DEMIRAY (1976) and JANZ *et al.* (1976) have provided finite elasticity spherical left-ventricular models whose constitutive properties are characterised in terms of the parameters of the left-ventricle medium's strain energy density function. Therein, by solving the equilibrium equations (with associated boundary conditions) the constitutive parameters are expressed and determined in terms of the monitored chamber pressure and volume.

GHISTA (1974) characterised the myocardial constitutive properties by relating the corresponding elements of the instantaneous stress and strain tensors of an ellipsoidal shaped left ventricular chamber by means of the Hill type 3-parameter constitutive model comprising of series elasticity, parallel elasticity and the contractile elements. The stresses were obtained in terms of the instantaneous chamber geometry and pressure by invoking elasticity theory. The strains were obtained from cineangiocardiographic data of the dynamic geometry of the left ventricle. Thus the values of the constitutive elements were obtained in terms of monitored instantaneous chamber pressure and dimension data.

The model was applied to clinical data, and *in vivo* representations of series elasticity, parallel elasticity and the contractile elements were obtained (for the first time, to the author's knowledge), as illustrated in Fig. 1. The model's potential in employing this illustrated contractile element characteristics as an average measure of myocardial contractility characteristics has (to our knowledge) not been explored. Conceivably, more representative myocardial characteristics can be obtained by employing, instead of the Hill's 3-parameter constitutive model, an alternative 3-element model (GLANTZ, 1977) wherein the series and parallel elastic elements are replaced by nonlinear viscoelastic elements and the contractile element is force dependent (i.e. to the number of cross bridges) and not length dependent. This recent constitutive model of Glantz provides better qualitative agreement with known sacromere biophysics.

Nevertheless, this model, as well as all the above

mentioned ones, suffers from not being able to yield regional variations in the contractile properties of the myocardium. The constitutive properties, so obtained, are some sort of average properties for the entire left ventricle, and at most help provide a gross evaluation of the normal-pathological state of the left ventricle. It is more useful to obtain the regional distribution of the constitutive properties of the left ventricle, so as to help delineate pathological myocardial segments. This paper presents the

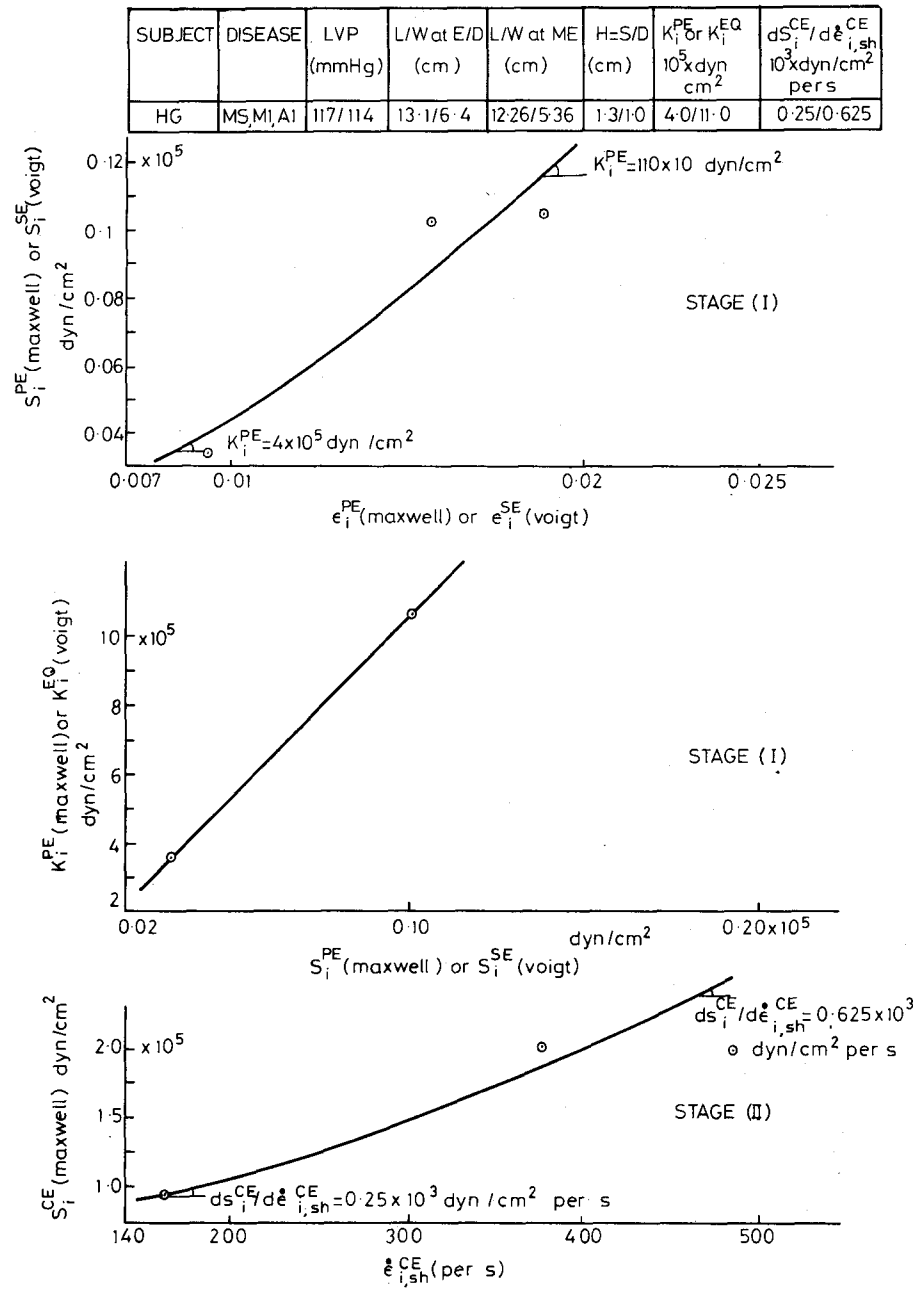

Fig 1 In vivo *determined values of the constitutive characteristics of the series elastic and contractile elements of the 3-element constitutive model of Ghista (1974). Note the strain dependence of the stress in the series and parallel elastic elements and the strain rate dependence of the stress in the contractile element. The values of their constitutive indices (which could have some pertinent physiological correlations and clinical implications) are given in the table of the figure*

development and clinical application of such a model.

3 New-approach to noninvasive detection of diseased myocardial elements by l.v.-mechanomyography (l.v.-m.m.c.g.)

The drawbacks of some of the models of cardiac mechanical functional assessment are (i) assumption of an idealised geometry for the left ventricular chamber, (ii) an overall index for the entire left ventricular myocardium, (iii) lack of an index for the assessment of left-ventricular pumping efficiency. To overcome these deficiencies, we have developed a totally new approach towards the non-invasive determination of (*a*) regional properties of the myocardium during diastole and delineation of the location and extent of diseased myocardial elements, and (*b*) the blood-pressure distribution in the left ventricular chamber at ejection time, as indices of its pumping efficiency and of the efficacy of coronary bypass surgery. As indicated before, in this paper (part 1) we will provide the regional myocardial properties during diastole (by the l.v.-m.m.c.g. method). Then, in part 2, we will compute the blood-pressure distributions, in the chamber, at systole, and demonstrate the development of contractility indices therefrom.

We have also called our two techniques by patent names, so as to help introduce them into the clinical arena. Accordingly, the technique for determination of the regional properties of the left-ventricular myocardium is called l.v.-mechanomyography. The method for determination of the left ventricular chamber's pressure and velocity distribution is called l.v.-pressovelography (which will be presented in part 2 of this paper). In the following subsection we will provide the foundations and clinical application of l.v.-mechanomyography.

3.1 *Aim*

Our aim here is to determine the mechanical constitutive properties of the various myocardial elements of the left ventricular chamber during diastole. The constitutive property of an element can be expressed in terms of a nonlinear stress (σ)-strain (ε) relationship, such as $\sigma = (a, b)\,[\exp(b\varepsilon) - 1]$ or alternatively as a linear Young's modulus (E)-stress (σ) relationships:

$$E = a + B\sigma$$

This means that we need to determine the values of the sets (E, σ), for the myocardial elements, so that the values of the constitutive parameters 'a' and 'b' could be determined.

3.2 *Requisite data utilisation and the overall approach*

The data, that we have available, are (i) the dynamic geometry of the left ventricular chamber which, although currently obtainable from cine-angiocardiography, can be made available from 2-dimensional echocardiography (ANDERSON *et al.*, 1977) and (ii) chamber pressure, as monitored by a catheter-tip manometer or a fluid-filled catheter manometer. From the sequential instantaneous endocardial outlines of the left ventricle, we obtain the instantaneous deformation of the endocardial boundary of the left ventricle, by assuming that points $Y^*_{i,n}$ on the endocardial boundary, formed by its intersection with the ith chord (normal to major chord, joining the midpoint of the base or the point on the common edge of the aortic and mitral valves with the apex), at instant t_n traverse to points $Y^*_{i,n+1}$ on the endocardial boundary at instant t_{n+1}. This formulation, illustrated in Fig. 2, is based on the experimental studies of INGELS *et al.* (1975).

From the above information, we will determine the instantaneous modulus E_n and the incremental myocardial stress $\Delta\sigma_n$ due to the incremental chamber pressure loading P_n, between successive instants, (ii) plot E_n against $\sigma_n(= \sum_n \Delta\sigma_n)$ on the (E, σ) co-ordinate plane, (iii) fit eqn. 1 to the plotted set of points, (iv) determine the ranges of values of (a, b) and hence of (E, σ) domains for both healthy and infarcted myocardium. Thus for any subject who is studied, we can, by determining the values of the left-ventricular myocardial segments' (E_n, σ_n) detect whether those segments are healthy or infarcted.

3.3 *Methodology*

In the framework of this paper, we will confine ourselves to the determination of the instantaneous values of E_n and σ_n (and hence of a and b), for the passive myocardium, i.e. during diastole. The requisite stepwise procedure entails: (*a*) the development of a finite-element model for the instantaneous

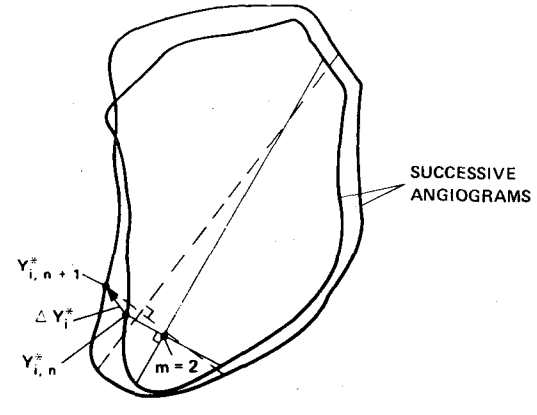

Fig. 2 Schematic illustration of the mode of translation of individual points on the left ventricular endocardial boundary (as experimentally observed by Ingles et al. (1975). This concept is employed to determine the instantaneous left ventricular endocardial displacements

geometry of the left ventricle provided in Section 3.4; (*b*) expressing, by means of the model, the instantaneous inner-wall displacement $\Delta Y^m_{i,n}$ of the instantaneous left ventricular chamber at the co-ordinate points $Y_{i,n}$ at time t_n, in terms of the unknown but initially assumed values instantaneous moduli $E = E_n$ or E_{ne} of the '*e*' elements, and the known incremental pressure acting on the wall of the left ventricular chamber; (*c*) obtaining the actual instantaneous wall displacements $\Delta Y^a_{i,n}$ (as described by the experimentally based formulation of Fig. 2), comparing these values with those of the *in vivo* displacements by evaluating the following criterion:

$$f(E_{ne}) = \{\sum_i [\Delta Y^m_{i,n}(E_{ne}) - \Delta Y^*_{i,n}]^2\}^{\frac{1}{2}} \leqslant \varepsilon, \quad \text{a small tolerance value} \qquad (2)$$

(*d*) reassigning the values of E_{ne} and converging to their optimal values which satisfy the above criteria, by means of an iterative optimisation procedure that is illustrated in Fig. 3 and discussed in the following Section; (*e*) determining the values of the associated instantaneous incremental myocardial elemental stress $\Delta\sigma_{ne}$ (for the optimal set of values of E_{ne}) corresponding to instant t_n; (*f*) calculating the set of values of the total instantaneous myocardial element stress σ_{ne} $(= \sum_n \Delta\sigma_{ne})$ and the associated E_{ne}, for at least three instants during diastole, and determining the values of *a* and *b* (eqn. 1), for the best straight line fits through the plotted sets of points and (E_{ne}, σ_{ne}), on the (E, σ) co-ordinate plane (note that both E_{ne} and σ_{ne} correspond to the instantaneous chamber geometry and chamber pressure).

3.4 3-*dimensional finite-element model of the left ventricle for l.v.-mechanomyocardiography*

The 3-dimensional left ventricular chamber geometry associated with a particular instant or frame is reconstructed, from its monitored 2-dimensional A–P (anterior–posterior) projection image, by the method indicated earlier by GHISTA *et al.* (1977). The cross-sections of this 3-dimensional reconstruction, taken normal to its imaged A–P plane projection and to the major chord (of the A–P image) connecting the midpoint of the aortic valve to the apex, are ellipses whose major axes lie in the A-P plane (and hence are measured from the A–P image) and whose minor axes (located in the lateral plane) are 0·9 times the lengths of the measured major areas. The 3-dimensional chamber is then discretised by means of 8-node hexahedral-type elements, each of which is composed of 5-node tetrahedral elements (ZIENKIEWICZ, 1971), with

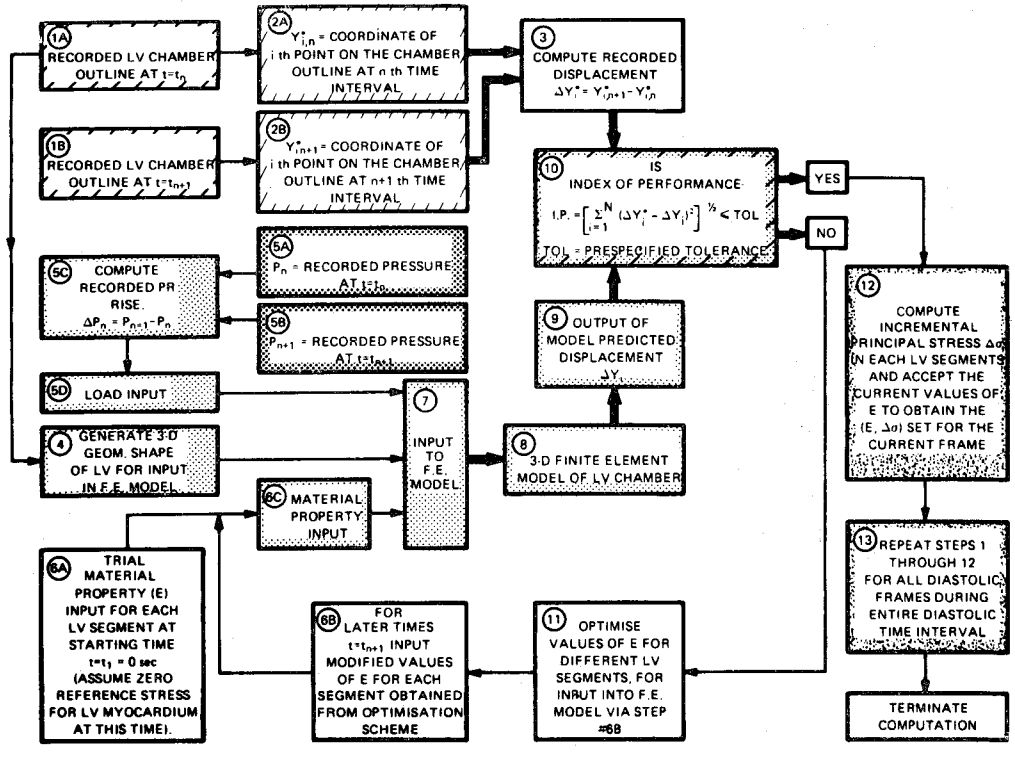

Fig. 3 The flow chart delineating the iterative procedure of matching the left ventricular model deformations with those of the monitored deformations at instant t_n to determine the values of the myocardial elements' Young's modulus E_n and the principal stress σ_n

nodes i, j, k, l. The co-ordinates of a typical nodal point i of a tetrahedral element are given by (x_i, y_i, z_i), whereas a typical point p inside the tetrahedron is represented by the co-ordinate x, y, z).

The relationship between the global Cartesian co-ordinates and the local 'natural co-ordinates' is given by

$$\begin{bmatrix} x \\ y \\ z \\ 1 \end{bmatrix} = \begin{bmatrix} x_i & x_j & x_k & x_l \\ y_i & y_j & y_k & y_l \\ z_i & z_j & z_k & z_l \\ 1 & 1 & 1 & 1 \end{bmatrix} \begin{bmatrix} L_i \\ L_j \\ L_k \\ L_l \end{bmatrix} \quad . \quad . \quad (1)$$

wherein

$$\begin{bmatrix} L_i \\ L_j \\ L_k \\ L_l \end{bmatrix} = \frac{1}{6V} \begin{bmatrix} a_i & b_i & c_i & d_i \\ a_j & b_j & c_j & d_j \\ a_k & b_k & c_k & d_k \\ a_l & b_l & c_l & d_l \end{bmatrix} \begin{bmatrix} 1 \\ x \\ y \\ z \end{bmatrix} \quad . \quad (2)$$

V is the volume of tetrahedron, and (a_i, b_i, c_i and d_i) are expressed in terms of their nodal co-ordinate as

$$a_i = \begin{vmatrix} x_j & y_j & z_j \\ x_k & y_k & z_k \\ x_l & y_l & z_l \end{vmatrix} ; \quad b_i = \begin{vmatrix} 1 & y_j & z_j \\ 1 & y_k & z_k \\ 1 & y_l & z_l \end{vmatrix}$$

$$c_i = -\begin{vmatrix} x_j & 1 & z_j \\ x_k & 1 & z_k \\ x_l & 1 & z_l \end{vmatrix} ; \quad d_i = -\begin{vmatrix} x_j & y_j & 1 \\ x_k & y_k & 1 \\ x_l & y_l & 1 \end{vmatrix} \quad (3)$$

To maintain the appropriate signs of the above equations, the right-hand system of numbering the nodes is maintained throughout the program.

3.4.1 *Displacement field of the tetrahedral element*

The assumed displacement field of the tetrahedral element is obtained by linear interpolation between nodes, and is given in terms of the natural co-ordinates given in eqn. 2 by

$$\{\delta\} = \begin{Bmatrix} u \\ v \\ w \end{Bmatrix} = \begin{Bmatrix} \sum_{n=i}^{l} N_n(x, y, z)\, u_n \\ \sum_{n=i}^{l} N_n(x, y, z)\, v_n \\ \sum_{n=i}^{l} N_n(x, y, z)\, w_n \end{Bmatrix} = \begin{Bmatrix} [N]\{u\} \\ [N]\{v\} \\ [N]\{w\} \end{Bmatrix} \quad . \quad . \quad . \quad (4)$$

where

$$[N] = [L_i\, L_j\, L_k\, L_l], \ \{u\} = \begin{Bmatrix} u_i \\ u_j \\ u_k \\ u_l \end{Bmatrix}, \text{ etc.} \quad . \quad (5)$$

3.4.2 *Strain-displacement relation*

The usual small strain/displacement relation is employed, namely

$$\{\varepsilon\} = [B]\{\delta\} \quad . \quad . \quad . \quad . \quad . \quad . \quad . \quad . \quad . \quad (6)$$

where

$$[B] = [B_i\, B_j\, B_k\, B_l] \quad . \quad . \quad . \quad . \quad . \quad . \quad . \quad . \quad (7)$$

and the typical term B_i is given by

$$[B_i] = \begin{vmatrix} L_{i,x} & 0 & 0 \\ 0 & L_{i,y} & 0 \\ 0 & 0 & L_{i\,z} \\ L_{i,y} & L_{i,x} & 0 \\ 0 & L_{i,z} & L_{i,y} \\ L_{i,z} & 0 & L_{i,x} \end{vmatrix} = \frac{1}{6V} \begin{vmatrix} b_i & 0 & 0 \\ 0 & c_i & 0 \\ 0 & 0 & d_i \\ c_i & b_i & 0 \\ 0 & d_i & c_i \\ d_i & 0 & b_i \end{vmatrix} \quad . \quad (8)$$

3.4.3 *Stress-strain relation*

Assuming linear elasticity and isotropy, the stress-strain relation for an element is given by

$$\{\sigma\} = [C]\{\varepsilon\} \quad . \quad . \quad . \quad . \quad . \quad . \quad . \quad . \quad . \quad (9)$$

where the material matrix $[C]$ is given by

$$[C] = \begin{bmatrix} C_{11} & C_{12} & C_{13} & 0 & 0 & 0 \\ & C_{22} & C_{23} & 0 & 0 & 0 \\ & & C_{33} & 0 & 0 & 0 \\ \text{Sym} & & C_{44} & 0 & 0 & \\ & & & C_{55} & 0 & \\ & & & & C_{66} & \end{bmatrix} \quad . \quad (10)$$

and

$$\left.\begin{aligned} C_{11} = C_{22} = C_{33} &= \frac{E(1-\nu)}{(1+\nu)(1-2\nu)} \\ C_{12} = C_{13} = C_{23} &= \frac{E}{(1+\nu)(1-2\nu)} \\ C_{44} = C_{55} = C_{66} &= \frac{E}{2(1+\nu)} \end{aligned}\right\} \quad . \quad (11)$$

where the Poisson's ratio (ν) is taken equal to 0·49.

3.4.4 *Minimum potential energy principle*

The potential energy functional is given by

$$\pi(u, v, w) = U - W \quad . \quad . \quad . \quad . \quad . \quad . \quad . \quad . \quad (12)$$

where U and W are, respectively, the strain energy and work done due to the pressure on the inner surface of the l.v. chamber. They are given by

$$U = 1/2 \int_{vol} \{\sigma\}^T\{E\}dv \quad \text{and} \quad W = \int \{P\}^T\{\delta\}ds.$$

By substituting eqns. 6 and 9 therein, we obtain

$$\pi = 1/2 \int_{vol} \{\delta\}^T[B]^T[C]\,[B]\{\delta\}dv - \int_s \{P\}^T\{\delta\}ds \quad (13)$$

where $\{P\}$ provides the components of the pressure normal to the endocardial surface.

On differentiating eqn. 13 with respect to the element displacements (u_i, v_i, w_i), we obtain the discretised equation for an element (at a given node i) as

$$\int_{vol} [B^e_i]^T\,[C^e]\,[B^e_i]\,\{\delta^e_i\}\,dv = \int_s [N^e_i]\,\{P^e_i\}\,ds \; . \quad (14)$$

Note that for the nodes which do not lie on the endocardial wall of the chamber, the right-hand side of eqn. 14 is automatically zero.

Eqn. 14 may be rewritten as

$$[K^e_i]\,\{\delta^e_i\} = \{F^e_i\} \quad . \quad . \quad . \quad . \quad . \quad . \quad . \quad . \quad (15)$$

where

$$[K^e_i] = \int_{vol} [B^e_i]^T\,[C^e]\,[B^e_i]\,dV \quad . \quad . \quad . \quad (16)$$

and

$$\{F^e_i\} = \int_s [N^e_i]\,\{P_i\}\,ds \; . \quad . \quad . \quad . \quad . \quad . \quad . \quad (17)$$

Once all the element stiffness matrices are formed according to eqns. 16 they are assembled to form the overall stiffness matrix (whose size would be 3mm × 3mm where m is the total number of nodal points) given by

$$K_{ij}\delta_j = F_j \quad . \quad . \quad . \quad . \quad . \quad . \quad . \quad . \quad . \quad (18)$$

where $i = j = 3m$. m being the total number of nodal points.

The solution of eqn. 18 yields the nodal deformations δ_j predicting the left-ventricular chamber deformation, where from the nodal displacements at the endocardial nodes (denoted by $\Delta Y^m_{t,n}$ in the text) are obtained. These in turn yield the chamber geometry at the t_{n-1} instant, and hence the change in chamber volume ΔV_n. The calculated ΔV_n can be alternatively employed to determine the myocardial elements' E values by matching the model and monitored values of the instantaneous changes in chamber volumes (instead of the endocardial deformations).

3.4.5 *Optimisation procedure*

It may be noted, from eqn. 8, that once the element configurations are specified, the $[B]$ matrix is completely specified. Also, in eqns. 10 and 11, the only variable in the material matrix $[C]$ is the elastic stiffness E. Hence, eqn. 16 may be rewritten as

$$[K^e_i] = E^e \int_{vol} [B^e_i]^T\,[C^{*e}_i]\,[B^e_i]\,dv$$

where

$$[C^{*e}_i] = \frac{1}{E^e}\,[C^e_i]$$

so that the model displacements $\Delta Y^m_{t,n}$ (and hence the function f in eqn. 2) can be expressed in terms of the values of the elements' moduli (E). The scheme for minimisation of the function f consists of two phases.

Phase 1: This phase assumes the function to be minimised is quadratic and has, in matrix notation, the form

$$f(\boldsymbol{x}) = f(0) = \boldsymbol{a}^T\boldsymbol{x} + (1/2)\boldsymbol{x}^T G\boldsymbol{x} \quad . \quad . \quad . \quad (19)$$

where

$\boldsymbol{x}$ = vector of variables ($nx1$)

$f(0)$ = the value of the function $f(\boldsymbol{x})$ at point $\boldsymbol{x} = 0$

a = vector of constants ($nx1$)

G = (nxn) symmetric positive definite matrix of 2nd-order partial derivatives

n = number of variables.

The gradient vector (the first-order partial derivative vector) of $f(\boldsymbol{x})$ is in the form

$$g(x) = \boldsymbol{a} + G\boldsymbol{x} \quad . \quad . \quad . \quad . \quad . \quad . \quad . \quad . \quad (20)$$

At the minimum of $f(\boldsymbol{x})$ we have

$$\boldsymbol{0} = \boldsymbol{a} = G\boldsymbol{h} \; . \quad . \quad . \quad . \quad . \quad . \quad . \quad . \quad . \quad . \quad (21)$$

where $\boldsymbol{h}$ is the value of x at the minimum.

Using this algorithm, we first calculate the function $f(\boldsymbol{x})$ at the point $\boldsymbol{x}_i$, which is

$$f(\boldsymbol{x}_i) = f(0) + \boldsymbol{a}^T\boldsymbol{x}_i + (1/2)\boldsymbol{x}^T_i\,G\boldsymbol{x}_i \; . \quad . \quad . \quad (22)$$

At the point $\boldsymbol{x}_{i+1} = \boldsymbol{x}_i + \Delta x$, eqn. 19 becomes

$$f(\boldsymbol{x}_{i+1}) = f(0) + a^T\boldsymbol{x}_{i+1} + (1/2)\boldsymbol{x}^T_{i+1}\,G\boldsymbol{x}_{i+1} \quad . \quad (23)$$

Substituting eqn. 22 into eqn. 23 and making use of eqn. 20 yields, after some manipulations,

$$f(\boldsymbol{x}_{i+1}) = f(\boldsymbol{x}_i) + g^T_i\,\Delta\boldsymbol{x} + (1/2)\Delta\boldsymbol{x}^T\,G\Delta\boldsymbol{x} \quad . \quad . \quad (24)$$

From eqn. 24 and the vector $\boldsymbol{g}$, the matrix G can be calculated by a centred-difference method. This calculation requires $n(n+3)/2+1$ function evaluations or $n(n+7)/2+1$ function evaluations for a better approximation. After evaluations of $\boldsymbol{g}$ and G, the following equation yields $\boldsymbol{h}$ the minimum of $f(\boldsymbol{x})$.

$$\boldsymbol{h} = \boldsymbol{x}_i - G^{-1}\,\boldsymbol{g}_i$$

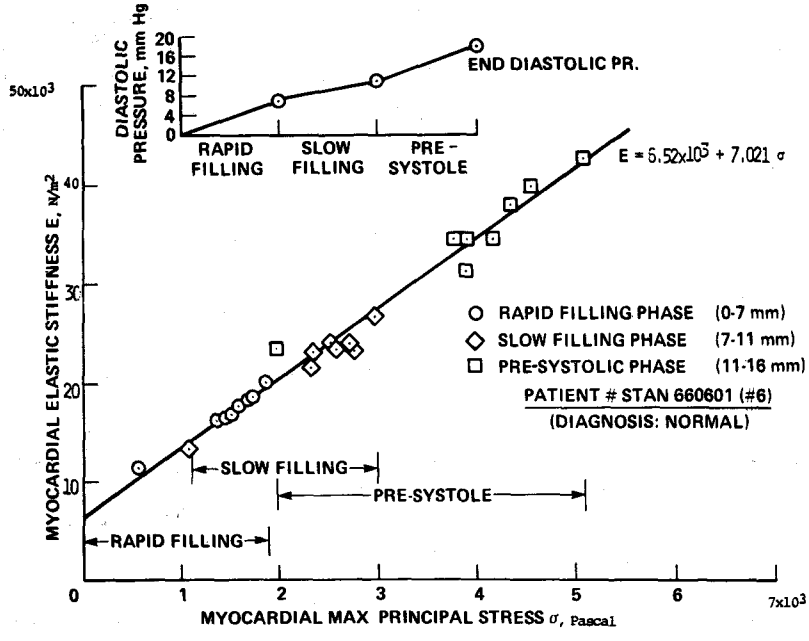

Fig. 4 Modulus (E) against principal stress relationship for the patient No. STAN 560601 with no myocardial disease symptoms

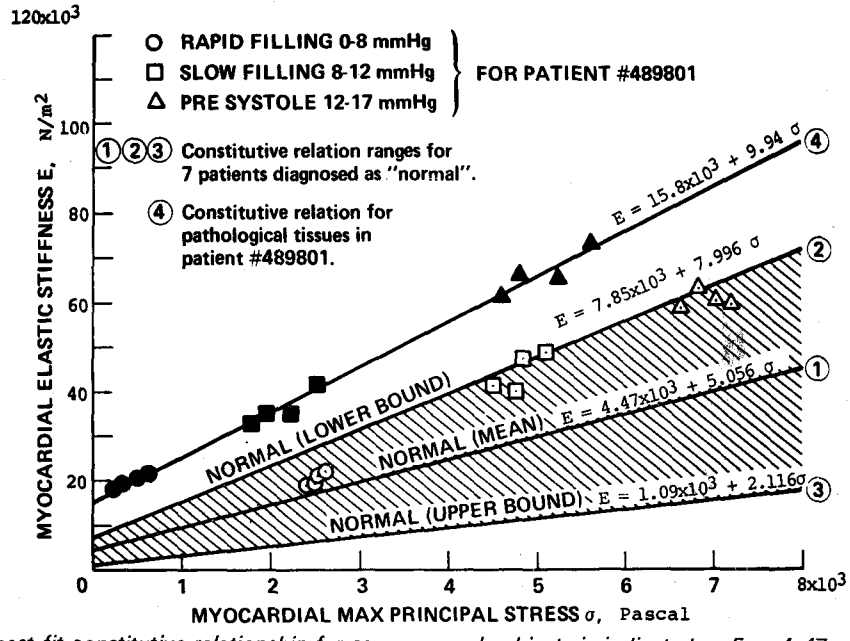

Fig. 5 The best-fit constitutive relationship for seven normal subjects is indicated as $E = 4{\cdot}47\times10^3+5{\cdot}056\sigma$ Nm^{-2}. In order to designate the normal myocardium's (E, σ) domain, the lower and upper bounds for the normal myocardium (whose mean property is $E = 4{\cdot}47\times10^3+5{\cdot}0565\sigma$ are designated at two standard deviations from this mean constitutive relationship. Now when the subject (No. 489801) having some myocardial disease symptoms is studied, some of the I.v. myocardial elements' (E, σ) fall outside the normal domain designated by the lower and upper bounds of Fig. 4; the remaining (four) elements fall within the normal domain

In most practical cases, the function $f(x)$ is not in the quadratic form of eqn. 9, therefore this method will yield the minimum only after a finite number of iterations.

Phase 2: In the second phase of this program, the given function is evaluated along the best path from the generic point $\boldsymbol{x}$ to $\boldsymbol{h}$, the minimum, based on the information gained in phase 1. The best path means the optimal direction for parametric variation to reach the minimum. Along this directional line, a second-order function is first used for interpolation to find the desired minimum. If it is not adequate, then either a third- or fourth-order function will be adopted to fit the function $f(\boldsymbol{x})$. The local minimum thus found will then be the starting point for the next iteration and so on until the index of performance is within the preset error tolerance.

4 Clinical results and implications

The above methods are applied to a number of cases of subjects who underwent cardiac catheterisation, for whom the chamber pressures were known. Some of these subjects (seven in number) were diagnosed as quasinormal while others (five in number) had myocardial infarction symptoms.

Fig. 4 gives the myocardial elastic modulus (or stiffness) E as a function of the maximum principal stress σ, for a subject with no symptoms of coronary lesions. The results are presented for eight major segments of the left ventricular chamber, during three different phases of diastole (namely early diastole, mid diastole and end diastole). It may be noted that, at any given instant during diastole, the stress state as well as the elastic modulus vary over the left ventricular myocardium. Further, as the filling progresses, the stresses and the corresponding elastic modulus increase, as noted by the (E, σ) co-ordinate points for the eight segments moving in batches to domains of higher values of E and σ. A straight line can be fitted through all the $E-\sigma$ data points, as $E = (6{\cdot}52\times10^3+7{\cdot}021\sigma)\ \mathrm{Nm}^{-2}$, providing a measure of the stress-dependent elastic modulus of the myocardium of the individual.

By following this procedure for seven assigned subjects with no symptoms of myocardial infarction, we obtain, as shown in Fig. 5, the mean and the upper and lower bounds of the modulus versus principal stress relationship (i.e. of the coefficients of the $E-\sigma$ relationship) of seven subjects who are clinically diagnosed as having a normal myocardium. These relationships (or the ranges of their coefficients) can now be utilised as bench marks to designate myocardial elements as normal or pathological. Now superimposed on the same Figure, we have plotted the myocardial (E, σ) values of a subject (No. 489801) who is diagnosed to have

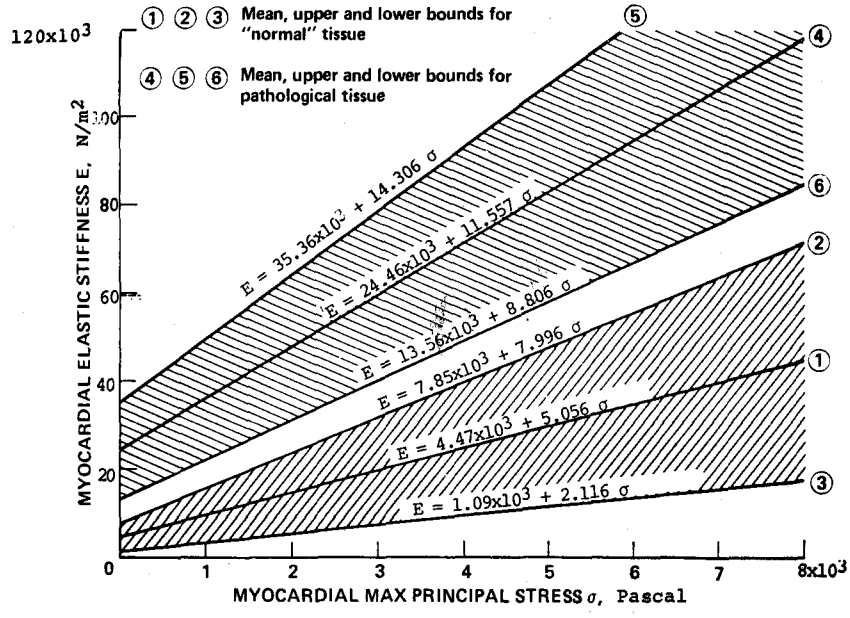

Fig. 6 For all those myocardial elements that do not fall within the designated normal domain, the best-fit, lower bound and upper bound constitutive relationships are determined as $E = 24{\cdot}46\times10^3+11{\cdot}557\sigma$, $E = 13{\cdot}56\times10^3+9{\cdot}8065\sigma$ and $E = 35{\cdot}56\times10^3+14{\cdot}306\sigma$. Thus, the infarcted myocardial domain is determined and designated to be distinctly separate from the 'normal' domain. Hence, by determining the instantaneous value of (E, σ) of a left ventricular myocardial element, and plotting the co-ordinate pair on the above $E-\sigma$ constitutive plane, we can determine if that element is normal or diseased

myocardial infarction symptoms. It is observed that (of the eight segments of the left ventricular chamber) the elastic constitutive ($E-\sigma$) properties of four of the left ventricular segments fall in the 'normal' range, while the other four segments (having an abnormally elevated stress dependent myocardial stiffness) fall outside this 'normal' range. The segments which are thus diagnosed to be pathological are numbered, so that they may then be properly depicted on the angiographic trace. Through those (E, σ) co-ordinates, that fall outside the normal $E-\sigma$ domain, a linear $E-\sigma$ is fitted to characterise the constitutive property of the pathological myocardium.

Fig. 6 now gives the mean, upper and lower bounds of all the values of (E, σ) of the five patients that fall outside the normal domain defined by Fig. 5. Because the domains of the normal and pathological elements are distinctly separate, one can clearly distinguish normal myocardial elements from those with coronary artery disease on the basis of their constitutive property co-ordinate sets (E, σ) falling within or outside the normal domain defined on the (E, σ) co-ordinate plane in Fig. 10.

References

ANDERSON, W. A., ARNOLD, J. T., CLARK, L. D., DAVIDS, W. T., HILLARD, W. J., LEHR, W. J. and ZITELLI, L. T. A new real-time phase-array sector scanner for imaging the entire adult heart. *Ultrasound in Medicine*, **3B,** 1547–1558.

BAKER, C. M. and PILKINGTON, T. C. (1974) The use of time dependent models in inverse electrocardiography. *IEEE Trans.*, **BME-21,** 460–468.

DEMIRAY, H. (1976) Stresses in ventricular wall. Paper No. 76-APM-31, ASME Meeting, Utah, June, 1976.

GHISTA, D. N. and VAYO, H. W. (1969) The time varying elastic properties of the left ventricular muscle', *Bull. Math.* Biophys., **31,** 75–92.

GHISTA, D. N. (1974) Rheological modelling of the intact left ventricle. In *Cardiac Mechanics* (Eds. I. MIRSKY, D. N. GHISTA and H. SANDLER, Wiley–Interscience, New York.

GHISTA, D. N., SANDLER, H. and VAYO, W. H. (1975*a*) Elastic modulus of the human intact left ventricle-determination and physiological interpretation. *Med. and Biol. Eng.*, **13,** 151–161.

GHISTA, D. N., RAO, B. H. and ADVANI, S. H. (1975*b*) *In vivo* elastic modulus of the left ventricle: its determination by means of a left ventricular model and its physiological significance and clinical utility. *Med. and Biol. Eng.*, **13,** 162–170.

GHISTA, D. N. and HAMID, S. (1977) Finite element analysis of the human left ventricle. *Computer Programs in Medicine*, **7,** 219.

GLANTZ, S. A. (1977) A three-element description of a muscle with viscoelastic passive elements. *J. Biomech.*, **10,** 5–20.

HARRISON, D. C., SANDLER, H. and MILLER, H. A. (1975) Cardiovascular, imaging and image processing—theory and practice. Society of Photo-optical instrumentation engineers, Palo Verdes Estates, California, 245–302.

INGLES, N. B., DAUGHTERS, G. T., STINSON, E. B. and ALDERMAN, E. L. (1975) Measurement of midwall myocardial dynamics in intact man by radiography of surgically implanted markers. *Circulation*, **52,** 859–867.

JANZ, R. F., KUBERT, B. R., MIRSKY, I., KORECKY, B. and TAICHMAN, G. C. (1976) Effect of age on passive elastic stiffness of rat heart muscle. *Biophys. J.*, 281–290.

MIRSKY, I., (1973) Ventricular and arterial wall stress based on large deformation analyses. *Biophys. J.*, **13,** 1141–1159.

NIKRAVESH, E. P. (1976) Optimisation in finite element analysis, with special reference to 3-dimensional left ventricular dynamics. Ph.D. thesis, Tulane University.

PAO, Y. and RITMAN, E. C. (1977) Global's Young modulus of urethane plastic cast of left ventricular myocardium calculated from Roentgen angiographic silhouettes. **10,** 133–140.